

RESEARCH PAPER

In-Situ Reactive Synthesis of Full Dense $\text{Si}_2\text{N}_2\text{O}$ by Incorporating of Amorphous Nanosized Si_3N_4 ; Effect of MgO and Y_2O_3

Mohammad Rezazadeh¹, Rahmatoallah Emadi¹, Ahmad Saatchi², Ali Ghasemi³

¹ Department of Materials Engineering, Isfahan University of Technology (IUT), Isfahan, Iran

² Materials Science and Engineering Department, University of Wisconsin- Madison, USA

³ Department of Materials Engineering, Malek Ashtar University of Technology, Shahin-Shahr, Iran

ARTICLE INFO

Article History:

Received 27 October 2018

Accepted 04 December 2018

Published 01 January 2019

Keywords:

Reaction sintering

$\text{Si}_2\text{N}_2\text{O}$

Si_3N_4 nanopowder

Spark plasma sintering

ABSTRACT

$\text{Si}_2\text{N}_2\text{O}$ is considered as a new great potential structural/functional candidate in place of Si_3N_4 . The amorphous Si_3N_4 nanopowder was incorporated into silica sol by adding of MgO and Y_2O_3 as sintering aid. Synthesized powders were heated by spark plasma sintering at a heating rate of 100 °C/min yielded fully dense compacts at 1550 and 1750 °C for 40 min. The phase formation of samples was characterized by X-ray diffraction technique and Raman spectroscopy. The microstructure was studied by field emission scanning electron microscopy equipped by energy dispersive X-ray spectroscopy. Optical emissivity of $\text{Si}_2\text{N}_2\text{O}$ phase was investigated by photoluminescence spectroscopy. The obtained results confirm that employing MgO in compare to the Y_2O_3 could promote the fabrication of a fully dense pure $\text{Si}_2\text{N}_2\text{O}$ specimen by SPS at much shorter time than conventional sintering. $\text{Si}_2\text{N}_2\text{O}$ have a strong, stable blue emission band centered at 455 nm with excitation wavelengths of 240 nm.

How to cite this article

Rezazadeh M, Emadi R, Saatchi A, Ghasemi A. *In-Situ Reactive Synthesis of Full Dense $\text{Si}_2\text{N}_2\text{O}$ by Incorporating of Amorphous Nanosized Si_3N_4 ; Effect of MgO and Y_2O_3* . *J Nanostruct*, 2019; 9(1):131-140. DOI: 10.22052/JNS.2019.01.014

INTRODUCTION

Compounds in the Si–O–N system exhibit excellent thermal, chemical, and mechanical stability, as well as high diffusion barrier and good dielectric properties [1]. Silicon oxynitride ($\text{Si}_2\text{N}_2\text{O}$) is a unique compound in the Si_3N_4 – SiO_2 system and reflects an excellent oxidation resistance at severe conditions for high temperature structural purposes [2–4].

In addition, it possesses very low theoretic density (2.81 g/cm³), high hardness (HV: 17–22 GPa), low thermal expansion coefficient (3.5×10⁻⁶ K⁻¹), good thermal shock resistance and high thermodynamic stability temperature (about 1800 °C) [5–8]. Recently, based on ab initio calculations, Goumri-Said et al. [9] predicted that $\text{Si}_2\text{N}_2\text{O}$ possessed low dielectric constant. However, there

* Corresponding Author Email: m.rezazadeh@ma.iut.ac.ir

are not enough experimental results to evaluate this conclusion mainly because of difficulty of the bulk $\text{Si}_2\text{N}_2\text{O}$ synthesis.

The reaction sintering process of $\text{Si}_2\text{N}_2\text{O}$ is close to the sintering of Si_3N_4 , i.e. both materials have strongly covalent bonds and low diffusion coefficient, requiring high sintering temperatures. This usually implies that oxide additives are needed to form a liquid phase with a eutectic melting point low enough to permit sintering without excessive dissociation [10]. Pressureless sintering (PLS) lead to formation of $\text{Si}_2\text{N}_2\text{O}$ phase with purity of 80% by using equimolar mixture of SiO_2 and Si_3N_4 with appropriate additives after heating in a long time under N_2 atmosphere, in the best of circumstances [11]. Tong et al. [12] could synthesize the near theoretical density $\text{Si}_2\text{N}_2\text{O}$

samples with purity of 98% at low temperature (1550 °C) by hot pressing (HP) method.

Eventually, $\text{Si}_2\text{N}_2\text{O}$ is in-situ fabricated by nitridizing a powder mixture of Si and SiO_2 or via Self-Propagating High-temperature Synthesis (SHS) [13,14]. In this method, usually much of Si_3N_4 is produced during the fabrication process, as well as residual Si and SiO_2 due to incomplete reaction with each other. Properties of $\text{Si}_2\text{N}_2\text{O}$ will be remarkably influenced by minor amounts of other phases, such as Si_3N_4 , Si, SiO_2 and oxide additives [15]. Wu et al. [16] fabricate $\text{Si}_2\text{N}_2\text{O}$ ceramic without presence of any kind of secondary phases by in-situ reactive method with nitridizing a powder mixture of Si and SiO_2 and multi-step sintering approach. However, this method leads to $\text{Si}_2\text{N}_2\text{O}$ phase along with high percentage of porosity, which could affect the final properties.

Spark plasma sintering (SPS) is a new powerful pressure sintering method which applies high electrical energy in a short time directly to voids between powder particles and utilizes the high energy of plasma (generated momentarily by spark discharges between the particles) to achieve high thermal diffusion [14]. It is therefore capable of fabricate highly dense compacts at temperatures lower than those of conventional sintering methods in a short period of time which ranges between 5 and 20 min. There are several published previous literatures of SPS that discuss some of the recent advances that have occurred during the past few years in reactive synthesis of bulk materials by SPS [17-19].

In the present work, a highly dense $\text{Si}_2\text{N}_2\text{O}$ ceramic without existence any kind of secondary phases is fabricated by in-situ reactive synthesis by SPS. The influence of different oxide (MgO and Y_2O_3) additives on the formation of $\text{Si}_2\text{N}_2\text{O}$ powders was compared. Phase transformation and densification mechanisms in SPS process were also studied. Finally, the photoluminescence Properties of $\text{Si}_2\text{N}_2\text{O}$ phase was investigated.

MATERIALS AND METHODS

Fabrication of $\text{Si}_2\text{N}_2\text{O}$

In order to increase the contact of specific surface of the raw material and improve the additive distribution, mixing of raw materials was carried out as follows. Silica sol was prepared after mixing of 22.1 ml tetraethylorthosilicate (TEOS; Merck), 22.1 ml ethanol (96%<; Merck) and 250 ml distilled water. 4 ml HCl (Merck) and 25 ml HNO_3 (Merck) were added as catalysts. 2 wt% MgO (>99% purity; Aldrich Chemical Company) and 2 wt% Y_2O_3 (>99% purity; Aldrich Chemical Company) as sintering aids were dissolved in stirring solution after 30 min. Commercial nanosized amorphous Si_3N_4 powder (>99% purity, ~20 nm, BET surface area= 61.2 m^2/g ; HeFei Kaier Nanometer Technology Development Co., Ltd., Anhui, China) was added into stirred solution gradually. The compositions of the mixtures used are tabulated in Table 1.

After aging at 60 °C and formation of gel, specimens were dried at 80 °C. After being sieved, the powder was loaded into a graphite die with an inner diameter of 20 mm, and then sintered by SPS (SPS10-60, Iran) at a temperature of 1550°C and 1750°C (heating rate of 100 °C/min) for 40 min under 50 MPa uniaxial pressure under 0.1 MPa fluid nitrogen gas. Finally, samples were ground and then polished on both sides.

Characterization of $\text{Si}_2\text{N}_2\text{O}$

Relative bulk density of the samples are measured by Archimedes method using distilled water, and then the total porosity is calculated according to the relative density and theoretical density of the $\text{Si}_2\text{N}_2\text{O}$ (2.81 g/cm^3).

Microstructure and morphology were characterized by field emission scanning electron microscopy (FE-SEM, MIRA 3 TESCAN, South Korea) equipped with electron dispersive spectroscopy (EDS). Phase composition of the sintered samples is identified by X-ray diffraction (XRD, PW1800,

Table 1. Chemical composition (mol%) of the mixtures studied.

Specimen	Si_3N_4	SiO_2	MgO	Y_2O_3
AS	50	50	-	-
ASY	49	49	-	2
ASM	49	49	2	-

Philips, Netherlands). The X-rays were produced using a sealed tube and the wavelength of X-ray was 0.154 nm ($\text{CuK}\alpha$). The XRD traces were recorded in the 2θ range of 10-80° (step size of 0.04 and scan rate of 0.02°/min).

The distribution of secondary phase was studied using backscattered electron (BSE) detector with 0.1 atomic number resolution from the polished surface of samples.

Raman spectra were taken on dispersive Raman microscopy (BRUKER, Germany, model: Senterra) equipped with CCD detector and Laser wave number of 785nm. The photoluminescence (PL) emission and excitation spectra were recorded at a room temperature using a Shimadzu RF-5301 PC spectrofluoro-photometer. The excitation source was a Xenon lamp. The diameter of the beam focus was about 1 μm . According to calculated optical band gap of $\text{Si}_2\text{N}_2\text{O}$ (5.1 eV [20]), two excitation wavelengths 240 and 580 nm were selected to

study of photoluminescence properties.

RESULTS AND DISCUSSION

Structural features of synthesized specimens

Fig. 1 displays XRD patterns of MgO added synthesized powder. It was revealed from the pattern, that the structural features of synthesized powder are completely amorphous.

As mentioned above, oxide additives that make a liquid phase with the SiO_2 , should enhance the dissolution of Si_3N_4 and formation rate of $\text{Si}_2\text{N}_2\text{O}$. The type, amount and distribution of metal oxide additives determine the formation temperature, the quantity and viscosity of the liquid phase. Nevertheless, the proper distribution of additive lead to reduction of required sintering aids and sintering time to fully convert to $\text{Si}_2\text{N}_2\text{O}$. Fig. 2a shows FE-SEM micrograph of agglomerated synthesized powder. Dissolution of additive in SiO_2 solution is caused relatively uniform distribution

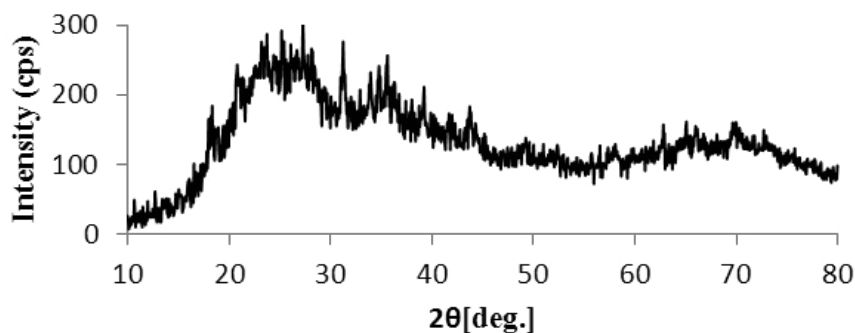


Fig. 1. XRD pattern of synthesized powder.

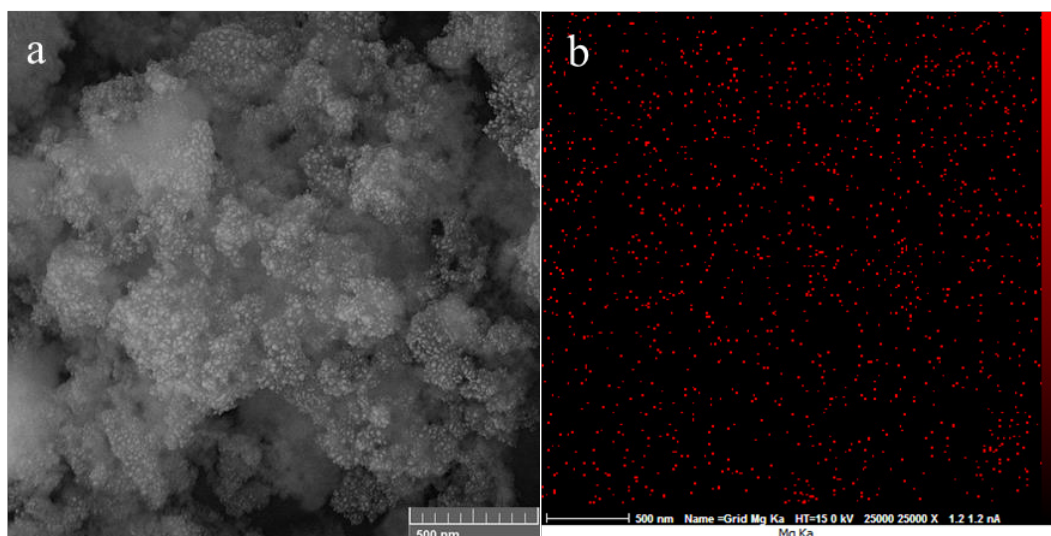


Fig. 2. (a) FE-SEM micrograph of synthesized powder with MgO additive, (b) EDS map of Mg atom .

(Fig. 2b). Uniform distribution of additives in silica sol and using of nanopowder could increase the surface contact of raw materials and improve the kinetic of reactions, finally.

Phase transformation in SPS process

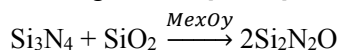
AS specimen

Based on the thermodynamic data, Si₂N₂O could formed above 1200 °C [15, 21]. However, the X-ray results for specimen AS indicates that no Si₂N₂O is formed at 1550 °C (see Fig. 3). It was revealed from the pattern that the sample consists of α-Si₃N₄ phase according to JPCDS card No. 09-0250 and moreover, β-Si₃N₄ (XRD JPCDS card No. 072-1308) as secondary phase and some remained glassy phase. Increasing the sintering temperature to 1750 °C caused to nucleation of Si₂N₂O (XRD JPCDS card No. 072-1307). Since, SiO₂ have the melting point higher than 1600 °C, consequently, viscous liquid is formed around Si₃N₄ powder. Si₃N₄ is dissolved and reacted with the Si-O liquid and Si₂N₂O nucleates and grows on the surface of remained Si₃N₄. Despite to the previous published literatures [11, 12, 22], Si₂N₂O was formed without additive in SPS process at a relatively short time. As regards Si-O viscous liquid at the temperature of 1750 °C, the growth of Si₂N₂O stops.

ASY specimen

Fig. 4 reflects XRD patterns of ASY specimen that is sintered at different temperature. As can be seen from the pattern, Si₂N₂O was formed as the secondary phase at temperature of 1550 °C, however after increasing temperature to 1750 °C, Silicon oxynitride phase was not formed.

In the presence of a liquid phase obtained by the addition of metal oxide (Me_xO_y), the formation reaction of Si₂N₂O can be described as the following reaction [12, 22]:



The synthesis/sintering process of Si₂N₂O involves a liquid phase sintering mechanism. A liquid phase is formed by reaction of the metal oxide additives and SiO₂. Then Si₂N₂O is formed through Si₃N₄ dissolving and reacting with the SiO₂ component of the liquid phase.

Unlike conventional sintering method, Si₂N₂O was formed by SPS at 1550 °C, without the presence of liquid phase. Fan et al. [23] was suggested a model for the crystallization mechanism of Si₂N₂O without any liquid phase from amorphous Si₃N₄ nanopowder in SPS process which, slightly modified, should be applicable in the present case. A part of nitrogen atoms in the

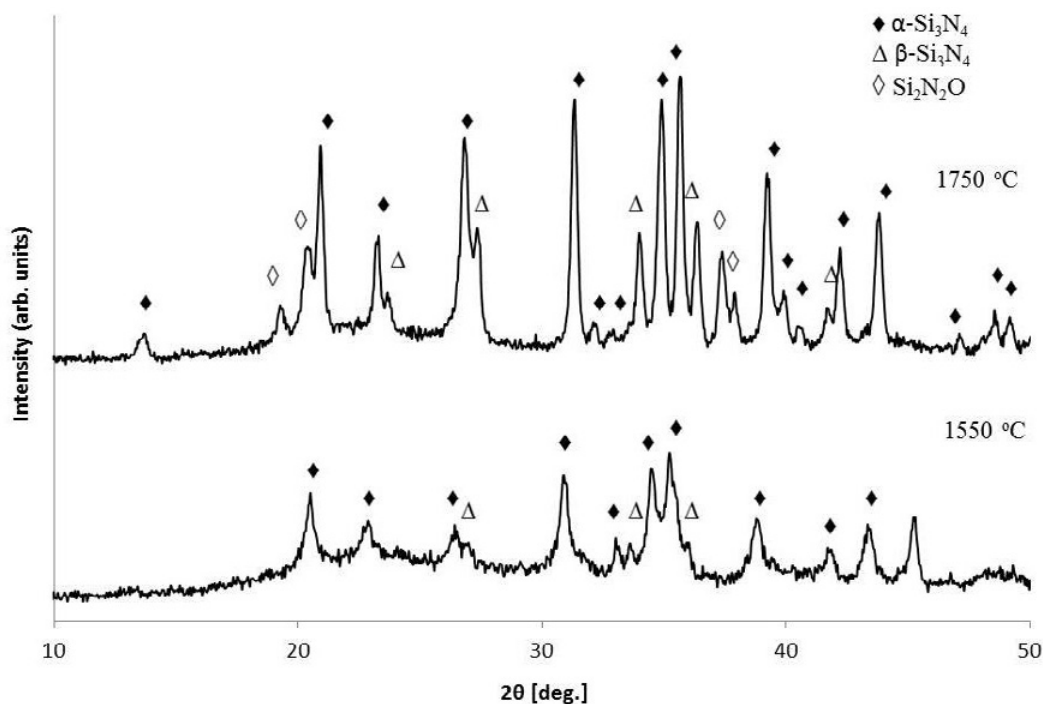


Fig. 3. XRD patterns of specimen AS sintered by SPS for 40 min at different temperature.

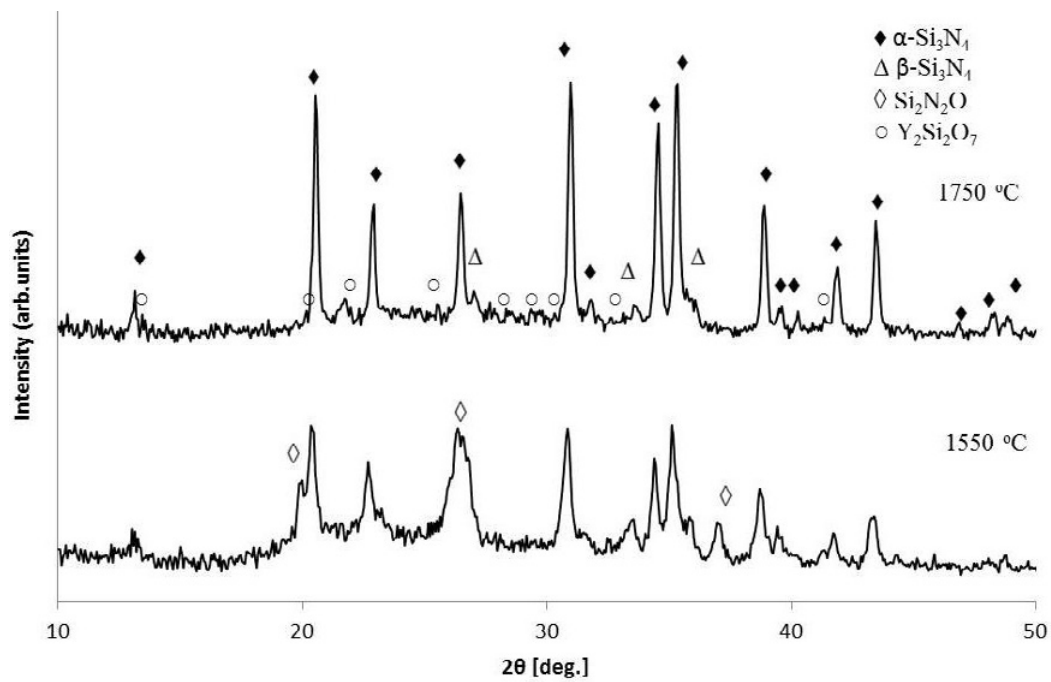


Fig. 4. XRD patterns specimen ASY sintered by SPS for 40 min at different temperature.

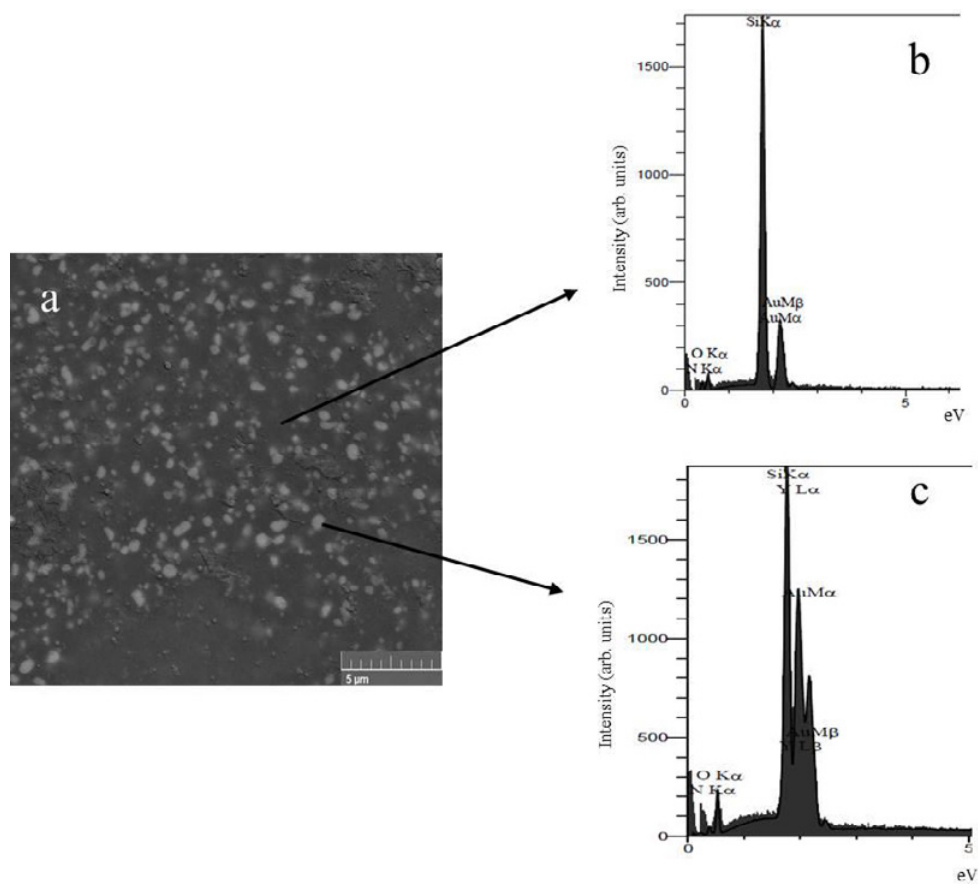


Fig. 5. (a) BSE micrograph from polished surface of ASY specimen after sintering at 1750 °C by SPS, EDS results from (b) dark background and (c) bright spots.

amorphous Si₃N₄ are replaced by the oxygen atoms presented in Y-Si-O dried sol, and consume in the process of sintering under vacuum. A mixed Si-N₄-O_n tetrahedra amorphous structure is formed by the diffusion of oxygen atoms into the inside of the amorphous Si₃N₄ powder, and the oxygen and nitrogen content are in gradient distribution. Therefore, Si₂N₂O crystals were nucleate at the position where the tetrahedra structure is similar to that of Si₂N₂O, and distribute discontinuously.

At higher temperature, Y₂Si₂O₇ phase was formed in the sample as a secondary phase beside Si₃N₄ phase (Fig. 4). Consequently, Si₂N₂O could not be formed at 1750 °C. BSE micrograph and EDS results from ASY polished surface are shown in Fig. 5. In this micrograph, bright spots can be considered in the dark background. The EDS results indicated that the bright spots have the yttrium. Traces of yttrium cannot be detected in dark area. So these results confirm the fact that Y₂O₃ with SiO₂, create a eutectic transformation higher than 1660 °C [24], and contribute to increase the density of the sample (3.2 g/cm³) because of the liquid sintering. Therefore, Y-Si-O dried sol was crystallized to Y₂Si₂O₇ after being sintered at 1750 °C and reactive sintering did not occurred. Accordingly, it seems no free oxygen

remained in structure to react with Si₃N₄.

ASM specimen

Fig. 6 shows XRD patterns of ASM specimen which is sintered at 1550 and 1750 °C for 40 min. Si₃N₄, Si₂N₂O and forsterite (Mg₂SiO₄) phases were identified after being sintered at 1550 °C. Comparing results with the specimens AS and ASY revealed that the presence of MgO could enhance the rate of reactive sintering and formation of Si₂N₂O in SPS. Si₂N₂O phase was formed completely and there is not any trace of raw materials for specimen ASM that have been sintered by SPS at 1750 °C. It appears clearly that the phase transformation progress is also very fast in the SPS process.

Fig. 7 gives the Raman spectra of the amorphous ASM synthesized powder and the sample sintered by SPS at 1750°C. The spectrum of the amorphous synthesized powder implies the lack of long range order. Three peaks at about 110, 181, and 251 cm⁻¹ are assigned to the Si₂N₂O compound [25]. The Raman peak at 458 cm⁻¹, assigned to amorphous SiO₂ [23]. So small amount of unreacted SiO₂ remain in structure that could not be detected based on the accuracy of the XRD pattern. The mechanism can be due to the lack of nitrogen in

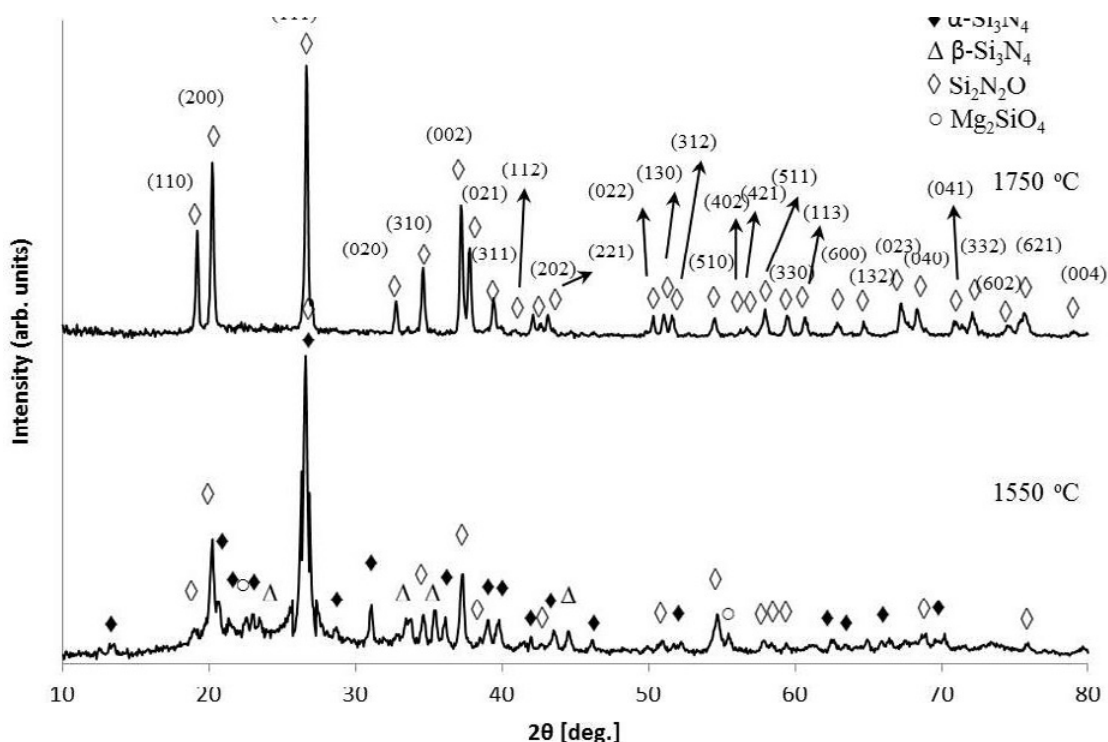


Fig. 6. XRD patterns of ASM specimen which is sintered at 1550 and 1750 °C for 40 min by SPS

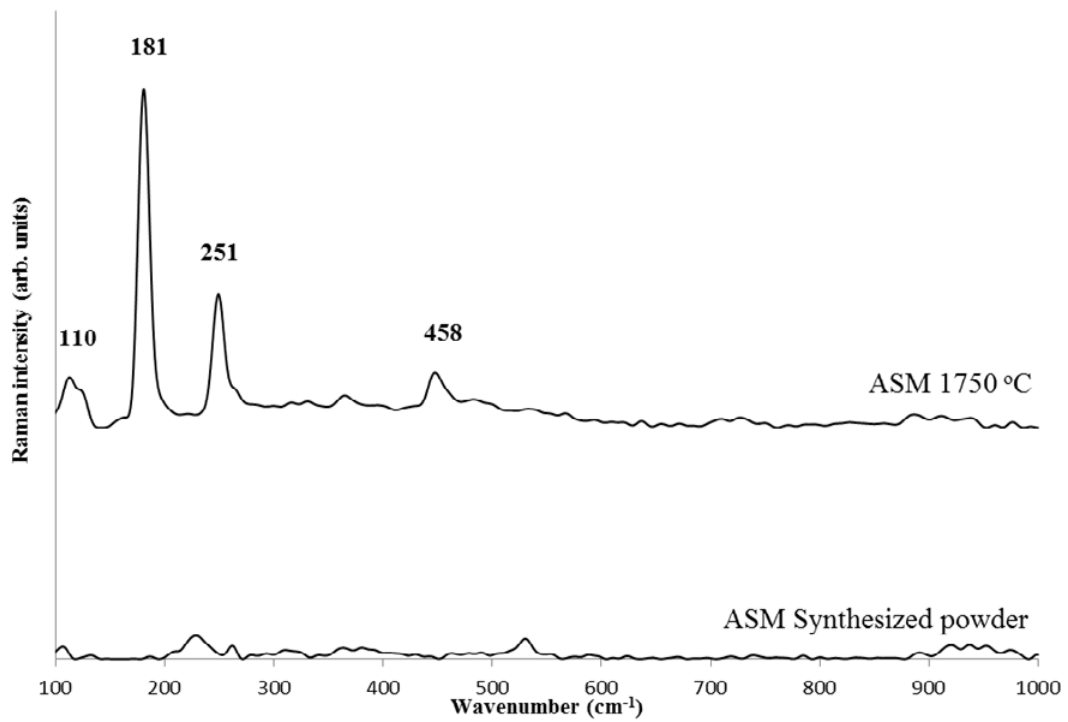


Fig. 7. Raman spectra of amorphous synthesized powder and ASM specimen sintered at 1750 °C by SPS.

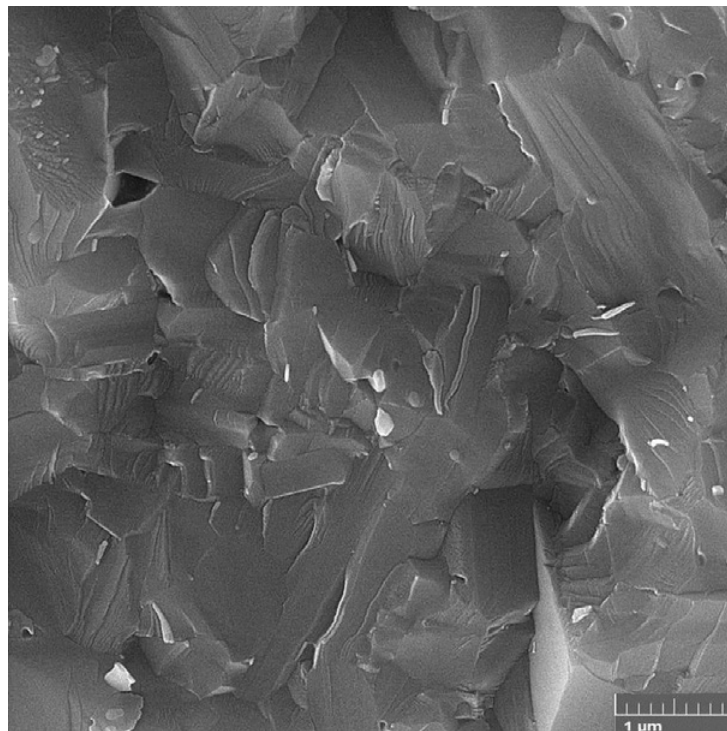


Fig. 8. FE-SEM micrograph of fracture surface ASM specimen after reaction sintering at 1750 °C for 40 min by SPS.

structure.

The density of ASM specimen was 2.8 g/cm³. It is very close to the theoretical density of $\text{Si}_2\text{N}_2\text{O}$ (>99.5% of theoretical density). FE-SEM micrograph of fracture surface of ASM specimen is shown in Fig. 8. So adding MgO could not only increase the reaction rate to the formation of pure $\text{Si}_2\text{N}_2\text{O}$ structure, but also creates a full density sample.

Mechanisms of formation of pure $\text{Si}_2\text{N}_2\text{O}$ in SPS process

The phase transformations/reactions that occur in the SPS process are controlled by the same mechanism as in conventional hot pressing. A solution-diffusion-precipitation mechanism with higher rate was taken place. This can be ascribed to the dissolution and diffusion processes being accelerated by the pulsed electric field. Wang et al. [26] have suggested a model for the microstructural evolution of the present system (ASM specimen). First, Si_3N_4 is dissolved into Si-Mg-O Liquid. Secondly, Once a sufficient supersaturation of the liquid is attained, $\text{Si}_2\text{N}_2\text{O}$ nucleates and quickly grows in the liquid, then, the degree of liquid supersaturation with (Si,N,O) is reduced, and the growth speed of $\text{Si}_2\text{N}_2\text{O}$ is therefore considerably decreased.

Upon the formation of a liquid phase based on Si-Mg-O, Si_3N_4 will dissolve into this liquid. It is known that the solubility of a particle in a liquid increases with reducing the size of the particle. Therefore, using of Si_3N_4 nanoparticle could enhance the rate of dissolution. These processes involve the reaction of Si_3N_4 grains and liquid phase interfaces, and diffusion of the (Si, N) ions in the liquid. It has been established that the former is the rate-controlling process [27]. Thus it can be generally expected that the time necessary for the liquid to become supersaturated will be controlled by the Si_3N_4 -liquid phase interface reaction.

Junting et al [28], have confirmed the complex crystallization and phase transition during the liquid phase sintering of amorphous nano-sized silicon nitride powders. At first, amorphous silicon nitride is converted to equiaxial $\alpha\text{-Si}_3\text{N}_4$. Then, after the formation of $\beta\text{-Si}_3\text{N}_4$ from $\alpha\text{-Si}_3\text{N}_4$, $\text{Si}_2\text{N}_2\text{O}$ heterogeneously nucleated on the surface of Si_3N_4 .

$\text{Si}_2\text{N}_2\text{O}$ can be described as being built up structurally by distorted SiN_3O tetrahedra, linked together to give an infinite three-dimensional network [29, 30]. Si and nitrogen atoms are

situated in an infinite two-dimensional puckered layer linked by an oxygen plane (typically the (200) plane). α - and $\beta\text{-Si}_3\text{N}_4$ are composed of SiN_4 tetrahedra. In Si_3N_4 , there similarly exists the Si-N puckered ring of infinite plane (typically such as the (1010) plane). Replacing nitrogen in a SiN_4 tetrahedron of Si_3N_4 by oxygen will give a unit of SiN_3O , which is the structural unit of $\text{Si}_2\text{N}_2\text{O}$. Thus it is quite reasonable to propose that any part of the surface of a $\beta\text{-Si}_3\text{N}_4$ grain which is in contact with the liquid will be eligible for formation of $\text{Si}_2\text{N}_2\text{O}$ on $\beta\text{-Si}_3\text{N}_4$ particle surfaces [26].

Because of the low solubility of Mg in $\text{Si}_2\text{N}_2\text{O}$ grains, growth of $\text{Si}_2\text{N}_2\text{O}$ embryos may induce the liquid surrounding these embryos to be rich in Mg. So the liquid viscosity is reduced locally, which in turn favors the growth of $\text{Si}_2\text{N}_2\text{O}$. This is currently described as the catalytic role of metal ions in the formation of $\text{Si}_2\text{N}_2\text{O}$.

According to the above description, proper distribution of metal ions in raw materials is the important factor to reducing the time required for fabrication of pure $\text{Si}_2\text{N}_2\text{O}$ specimen.

Densification mechanisms in SPS process

It is generally proposed that application of mechanical pressure promotes the removal of pores and enhances diffusion (as HP method). However, it is frequently argued that the promoted densification rates stem mostly from the use of direct high energy current pulses.

The fact that full density can be achieved with very limited involvement of phase transformation and grain growth suggests that densification is accomplished mainly via particle re-arrangement assisted by the presence of a liquid phase.

In this particular case, full density was approached within following stages. First, initial particle re-arrangement initiated when an oxygen-rich liquid is formed (MgO-SiO₂ eutectic liquid). Then Extensive particle re-arrangement effected by grain boundary sliding. And finally, closed pores will be eliminated. For SPS, the most attractive feature is the extensive second-stage particle re-arrangement that occurs dramatically fast.

As the sintering progresses so rapidly, it is easy to imagine that it is difficult for the liquid to equilibrate, implying that a nitrogen concentration gradient may exist momentarily in the liquid, close to the undissolved Si_3N_4 particles. The viscosity of such a liquid phase will depend strongly on the applied heating rate, because the liquid viscosity

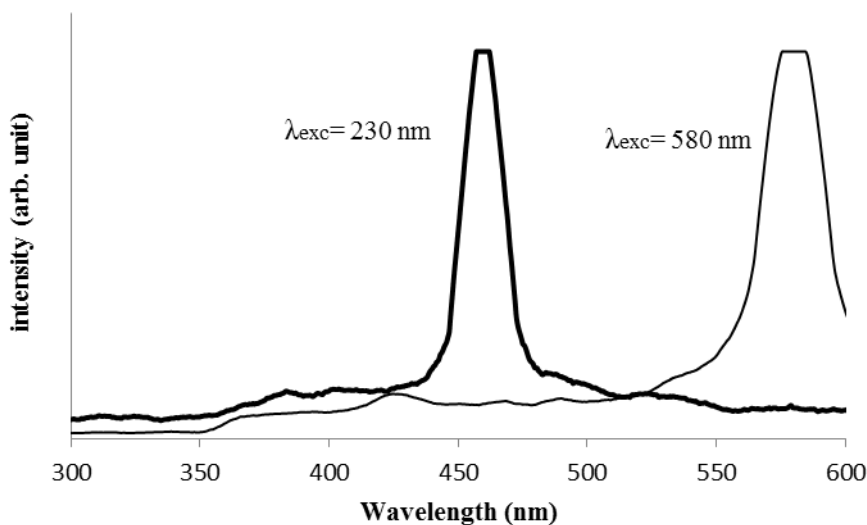


Fig. 9. PL spectrum of $\text{Si}_2\text{N}_2\text{O}$ with different excitation wavelength.

increases rapidly with increasing nitrogen content [31]. A high heating rate reduces the viscosity by raising the non-equilibrium oxygen rich part of liquid to higher temperatures [32, 33].

This phenomenon contributes to enhancing densification during SPS processing of silicon nitride-based ceramics. Due to the high heating rate applied, a concentration gradient is built up in the liquid, so that the liquid formed close to the Si_3N_4 particles is rich in nitrogen. When specimen rapidly heated, the oxygen-rich part of the liquid is brought up to a high temperature where it has very low viscosity, thus enhancing the particle sliding under compressive stress [34].

The SPS densification of $\text{Si}_2\text{N}_2\text{O}$ ceramics with MgO additive occurs within minutes, which is much faster than in conventional hot pressing.

Optical emissivity of $\text{Si}_2\text{N}_2\text{O}$

The photoluminescence (PL) properties of ASM specimen were started out at a room temperature with two excitation wavelengths of 240 nm and 580 nm (Fig. 9). This result shows that the $\text{Si}_2\text{N}_2\text{O}$ have a strong, stable blue emission band centered at 455 nm with excitation wavelengths of 240 nm, which is nearly symmetrical in shape. With lower excitation energy (lower than optical band gap) (580 nm), no PL peak is seen in PL spectrum of $\text{Si}_2\text{N}_2\text{O}$. Clearly, this emission were from a direct band gap emission and there are no deep-level or trap-level state in electronic structure of silicon oxynitride. These results are in a good agreement

with previous computational theoretical studies [1, 9, 20].

CONCLUSIONS

A spark plasma sintering process for fabrication of pure dense $\text{Si}_2\text{N}_2\text{O}$ ceramic was employed and the role of different oxide on the formation of silicon oxynitride was studied. Using of nanopowders and sol gel preparation method for mixing of raw materials lead to homogenous distribution of additives. Silicon oxynitride was formed as secondary phase in AS specimen without any additives. The fully dense pure $\text{Si}_2\text{N}_2\text{O}$ was fabricated with 2% mol MgO as an additive at 1750 °C after 40 min by SPS. The rapid densification is ascribed to extensive particle re-arrangement effected by grain boundary sliding, and to the creation of a non-equilibrium liquid phase by rapid heating. $\text{Si}_2\text{N}_2\text{O}$ have a strong, stable blue emission band centered at 455 nm with excitation wavelengths of 240 nm.

CONFLICT OF INTEREST

The authors declare that there are no conflicts of interest regarding the publication of this manuscript.

REFERENCES

1. Liu B, Wang J, Li F, Nian H, Zhou Y. Effect of interstitial lithium atom on crystal and electronic structure of silicon oxynitride. *Journal of Materials Science*. 2009;44(23):6416-22.
2. Dong X, Liu J, Du H, Guo A, Liu M. Microstructure

- characterization of in situ synthesized porous Si₂N₂O ceramics using spodumene additive. *Ceramics International*. 2013;39(4):4657-62.
3. O'Meara C, Sjöberg J, Dunlop G, Pompe R. Oxidation of pressureless sintered Si₂N₂O materials. *Journal of the European Ceramic Society*. 1991;7(6):369-78.
 4. Paul RK, Lee C-W, Kim H-D, Lee B-T. Microstructure characterization of in situ synthesized porous Si₃N₄-Si₂N₂O composites using feldspar additive. *Journal of Materials Science*. 2007;42(12):4701-6.
 5. Li X, Zhang L, Yin X. Study on in-situ reaction synthesis and mechanical properties of Si₂N₂O ceramic. *Ceramics International*. 2013;39(3):3035-41.
 6. Tong Q, Wang J, Li Z, Zhou Y. Preparation and properties of Si₂N₂O/β-cristobalite composites. *Journal of the European Ceramic Society*. 2008;28(6):1227-34.
 7. Bressiani JC, Izhevskiy V, Bressiani AHA. Development of the microstructure of the silicon nitride based ceramics. *Materials Research*. 1999;2(3):165-72.
 8. Ohashi M, Nakamura K, Hirao K, Toriyama M, Kanzaki S. Factors affecting mechanical properties of silicon oxynitride ceramics. *Ceramics International*. 1997;23(1):27-37.
 9. Goumri-Said S, Kanoun-Bouayed N, Reshak AH, Kanoun MB. On the electronic nature of silicon and germanium based oxynitrides and their related mechanical, optical and vibrational properties as obtained from DFT and DFPT. *Computational Materials Science*. 2012;53(1):158-68.
 10. Rocabois P, Chatillon C, Bernard C. Thermodynamics of the Si-O-N System: II, Stability of Si₂N₂O(s) by High-Temperature Mass Spectrometric Vaporization. *Journal of the American Ceramic Society*. 1996;79(5):1361-5.
 11. Bergman B, Heping H. The influence of different oxides on the formation of Si₂N₂O from SiO₂ and Si₃N₄. *Journal of the European Ceramic Society*. 1990;6(1):3-8.
 12. Tong Q, Wang J, Li Z, Zhou Y. Low-temperature synthesis/densification and properties of Si₂N₂O prepared with Li₂O additive. *Journal of the European Ceramic Society*. 2007;27(16):4767-72.
 13. Pradeilles N, Record MC, Marin-Ayral RM, Linde AV, Studenikin IA, Grachev VV. Influence of thermal conditions on the combustion synthesis of Si₂N₂O phase. *Materials Research Bulletin*. 2008;43(2):463-72.
 14. Radwan M, Kashiwagi T, Miyamoto Y. New synthesis route for Si₂N₂O ceramics based on desert sand. *Journal of the European Ceramic Society*. 2003;23(13):2337-41.
 15. Wu S, Li X. In-Situ Reactive Synthesis of Si₂N₂O Ceramics and Its Properties. *Metallurgical and Materials Transactions A*. 2012;43(12):4859-65.
 16. Wu S, Li X. Preparation of pure nano-grained Si₂N₂O ceramic. *International Journal of Refractory Metals and Hard Materials*. 2013;36:97-100.
 17. Wang L, Zhang J, Jiang W. Recent development in reactive synthesis of nanostructured bulk materials by spark plasma sintering. *International Journal of Refractory Metals and Hard Materials*. 2013;39:103-12.
 18. Orrù R, Licheri R, Locci AM, Cincotti A, Cao G. Consolidation/synthesis of materials by electric current activated/assisted sintering. *Materials Science and Engineering: R: Reports*. 2009;63(4-6):127-287.
 19. Munir ZA, Quach DV, Ohyanagi M. Electric Current Activation of Sintering: A Review of the Pulsed Electric Current Sintering Process. *Journal of the American Ceramic Society*. 2010;94(1):1-19.
 20. Zhang T, Wu M, Zhang S, Chen S, He M, Wang J, et al. Local electric field investigation of Si₂N₂O and its electronic structure, elastic and optical properties. *Journal of Alloys and Compounds*. 2011;509(5):1739-43.
 21. Hillert M, Jonsson S. Prediction of the Al-Si-N system. *Calphad*. 1992;16(2):199-205.
 22. Huang ZK, Greil P, Petzow G. Formation of silicon oxynitride from Si₃N₄ and SiO₂ in the presence of Al₂O₃. *Ceramics International*. 1984;10(1):14-7.
 23. Fan L, Shi Z, Lu X, Wang C, Chen M, Li Y, et al. Silicon Oxynitride Ceramics Prepared by Plasma Activated Sintering of Nanosized Amorphous Silicon Nitride Powder without Additives. *Journal of the American Ceramic Society*. 2013;96(8):2358-61.
 24. *Materials Fundamentals of Gate Dielectrics*. Springer-Verlag; 2005.
 25. Rouxel T, Besson J-L, Rzepka E, Goursat P. Raman spectra of Si₃AlON glasses and ceramics. *Journal of Non-Crystalline Solids*. 1990;122(3):298-304.
 26. Wang C, Emoto H, Mitomo M. Nucleation and Growth of Silicon Oxynitride Grains in a Fine-Grained Silicon Nitride Matrix. *Journal of the American Ceramic Society*. 2005;81(5):1125-32.
 27. Tsai RL, Raj R. Dissolution Kinetics of beta-Si₃N₄ in an Mg-Si-O-N Glass. *Journal of the American Ceramic Society*. 1982;65(5):270-4.
 28. Junting L, Kaifeng Z, Guofeng W, Wenbo H. Fabrication of fine-grained Si₃N₄-Si₂N₂O composites by sintering amorphous nano-sized silicon nitride powders. *Journal of Wuhan University of Technology-Mater Sci Ed*. 2006;21(3):97-9.
 29. Kroll P, Milko M. Theoretical Investigation of the Solid State Reaction of Silicon Nitride and Silicon Dioxide forming Silicon Oxynitride (Si₂N₂O) under Pressure. *Zeitschrift für anorganische und allgemeine Chemie*. 2003;629(10):1737-50.
 30. Wang CM, Pan X, Rhle M, Riley FL, Mitomo M. Silicon nitride crystal structure and observations of lattice defects. *Journal of Materials Science*. 1996;31(20):5281-98.
 31. Hampshire S. Oxynitride glasses, their properties and crystallisation – a review. *Journal of Non-Crystalline Solids*. 2003;316(1):64-73.
 32. Peng H, Shen Z, Nygren M. Reaction sequences occurring in dense Li-doped sialon ceramics: influence of temperature and holding time. *Journal of Materials Chemistry*. 2003;13(9):2285.
 33. Shen Z, Peng H, Nygren M. Rapid Densification and Deformation of Li-Doped Sialon Ceramics. *Journal of the American Ceramic Society*. 2004;87(4):727-9.
 34. Peng H. "Spark plasma sintering of Si₃N₄-based ceramics: sintering mechanism - tailoring microstructure - evaluating properties," *Institutionen för fysikalisk kemi, oorganisk kemi och strukturkemi, Univ., Stockholm*, 2004.